Genome Medicine

RESEARCH   **Open Access**

Developmental dynamics of voltage-gated sodium channel isoform expression in the human and mouse brain

Lindsay Liang[1], Siavash Fazel Darbandi[1], Sirisha Pochareddy[2], Forrest O. Gulden[2], Michael C. Gilson[1], Brooke K. Sheppard[1], Atehsa Sahagun[3], Joon-Yong An[4], Donna M. Werling[5], John L. R. Rubenstein[1], Nenad Sestan[2,6,7,8,9], Kevin J. Bender[3] and Stephan J. Sanders[1,10,11*]

Abstract

Background: Genetic variants in the voltage-gated sodium channels *SCN1A*, *SCN2A*, *SCN3A*, and *SCN8A* are leading causes of epilepsy, developmental delay, and autism spectrum disorder. The mRNA splicing patterns of all four genes vary across development in the rodent brain, including mutually exclusive copies of the fifth protein-coding exon detected in the neonate (5N) and adult (5A). A second pair of mutually exclusive exons is reported in *SCN8A* only (18N and 18A). We aimed to quantify the expression of individual exons in the developing human brain.

Methods: RNA-seq data from 783 human brain samples across development were analyzed to estimate exon-level expression. Developmental changes in exon utilization were validated by assessing intron splicing. Exon expression was also estimated in RNA-seq data from 58 developing mouse neocortical samples.

Results: In the mature human neocortex, exon 5A is consistently expressed at least 4-fold higher than exon 5N in all four genes. For *SCN2A*, *SCN3A*, and *SCN8A*, a brain-wide synchronized 5N to 5A transition occurs between 24 post-conceptual weeks (2nd trimester) and 6 years of age. In mice, the equivalent 5N to 5A transition begins at or before embryonic day 15.5. In *SCN8A*, over 90% of transcripts in the mature human cortex include exon 18A. Early in fetal development, most transcripts include 18N or skip both 18N and 18A, with a transition to 18A inclusion occurring from 13 post-conceptual weeks to 6 months of age. No other protein-coding exons showed comparably dynamic developmental trajectories.

Conclusions: Exon usage in *SCN1A*, *SCN2A*, *SCN3A*, and *SCN8A* changes dramatically during human brain development. These splice isoforms, which alter the biophysical properties of the encoded channels, may account for some of the observed phenotypic differences across development and between specific variants. Manipulation of the proportion of splicing isoforms at appropriate stages of development may act as a therapeutic strategy for specific mutations or even epilepsy in general.

Keywords: Isoform, Splicing, Voltage-gated sodium channel, Autism spectrum disorder, Intellectual disability, Developmental delay, Epileptic encephalopathy, Seizures, Exon 5A, Exon 5N

* Correspondence: stephan.sanders@ucsf.edu
[1]Department of Psychiatry and Behavioral Sciences, UCSF Weill Institute for Neurosciences, University of California, San Francisco, San Francisco, CA 94158, USA
[10]Institute for Human Genetics, University of California, San Francisco, San Francisco, CA 94158, USA
Full list of author information is available at the end of the article

Liang et al. Genome Medicine   (2021) 13:135

Page 2 of 14

Background

Genetic variation in the genes *SCN1A*, *SCN2A*, *SCN3A*, and *SCN8A* are a major cause of epileptic encephalopathy, autism spectrum disorder (ASD), and developmental delay [1–3]. These four homologous genes encode voltage-gated sodium channels ($Na_V1.1$, $Na_V1.2$, $Na_V1.3$, and $Na_V1.6$, respectively) that are critical for a range of functions in the central nervous system [4], including axonal action potential initiation and propagation [5, 6], dendritic excitability [7, 8], macroscopic anatomical development [9], and activity-dependent myelination [10]. The functional role, subcellular location, expression level, and isoform selection of voltage-gated sodium channels vary across development, and understanding this relationship is critical for understanding the etiology of the associated disorders and their therapeutic management [7, 11–19]. While some isoform-level differences have been assayed in rodents and mature human brains [15, 20–23], the trajectories in the developing human cortex have not been described [24].

Sodium channel genes are composed of multiple exons, which can be protein-coding (CDS for CoDing Sequence), untranslated regions (UTRs), or non-coding exons (NCEs). Gene isoforms are differing combinations of these exons, which can change the amino acid sequence of the encoded proteins (protein isoforms or proteoforms). The best-characterized isoform change across these four sodium channels are the two mutually exclusive copies of the fifth protein-coding exon [16, 25]. This exon encodes part of the first domain of the Na_V channel, including the end of transmembrane segment S3, most of transmembrane segment S4, and a short extracellular linker connecting these two segments (Fig. 1A). In humans, each copy of this fifth protein-coding exon is 92 nucleotides in length, encoding 30 amino acids, of which one to three amino acids vary between the two exon copies for each gene (Fig. 1B–E). "A" isoforms include the ancestral and canonical copy of exon 5 (5A), with an aspartic acid residue (Asp/D) encoded at position 7 of 30 [26]. "N" isoforms use the alternative copy of exon 5 (5N), with an asparagine residue (Asn/N) at position 7 of 30 in *SCN1A*, *SCN2A*, and *SCN8A* and a serine residue (Ser/S) in *SCN3A*. Despite this relatively small change in protein structure, differential inclusion of 5A or 5N can have marked effects on channel function. Indeed, these splice isoforms can alter channel electrophysiological characteristics [24, 27], the functional impacts of variants associated with seizure [24], neuronal excitability [28], response to antiepileptics [21, 22, 29], and seizure-susceptibility [28].

The utilization of the 5A or 5N varies across development, with 5N generally being expressed at higher levels in the neonatal period while 5A predominates in adults [30]. This switch is defined best in mouse, where the 5A:

5N ratio varies by gene and brain region along with developmental stage [20]. For *Scn2a* in mouse neocortex, the 5A:5N ratio is 1:2 at birth (postnatal day 0/P0) and flips to 3:1 by P15. For both *Scn3a* and *Scn8a*, 5A predominates throughout the postnatal period with a 2:1 ratio at P0 increasing to 5:1 by P15 [20]. *Scn1a* lacks a functional copy of 5N in the mouse genome. Similar developmental profiles currently have not been reported for humans beyond the 5A/5N utilization in *SCN1A* in adults, in which a 5A:5N ratio of over 5:1 was observed in the temporal cortex and hippocampus of adult surgical resections [21, 22].

In addition to the 5A/5N switch, a similar developmental shift in mutually exclusive exons has been reported for "exons 18A or 18N" in *SCN8A* only, regulated by the RNA-binding protein RBFOX1 [15, 23, 31]. Using GENCODE human v31 gene definitions [32], 18A maps to the 20th protein-coding exon of major *SCN8A* isoforms (CDS 20, Fig. 1A), while 18N encodes the 8th and last protein-coding exon (CDS 8) of a shorter transcript with eight protein-coding exons (ENST00000548086.3, Additional file 1: Fig. S1). In the embryonic mouse brain, most *SCN8A* transcripts include 18N or skip both 18N and 18A, leading to non-functional channels, while 18A predominates in the adult mouse and human brain [15, 23].

Here, we present data on the utilization of GENCODE-annotated protein-coding exons in four seizure-associated voltage-gated sodium channels in the human and mouse neocortex across development. We demonstrate a synchronized transition from 5N to 5A utilization between 24 post-conceptual weeks (2nd trimester) and six years of age across all four voltage-gated sodium channels and a transition from 18N to 18A in *SCN8A* from 13 post-conceptual weeks to 6 months of age. These isoform differences can modify the function of the encoded voltage-gated sodium channels, raising the potential that interventions, such as antisense oligonucleotides, could be used to modify the isoform ratio as a potential therapy for disorders caused by variants in sodium channel genes or epilepsy.

Methods

Genomic data

To quantify the relative proportion of protein-coding exon expression across development in the human cortex, we assessed bulk-tissue RNA-seq data from 176 *postmortem* neurologically normal samples of the dorsolateral prefrontal cortex (DLPFC, $N = 167$ older than 10 post-conception weeks) or frontal cerebral wall ($N = 9$ younger than 10 post-conception weeks) from the BrainVar cohort (Additional File 2: Table S1) [33]. These deidentified samples ranged from 6 post-conception weeks to 20 years of age with 104 males and 72 females. The BrainVar cohort also has corresponding whole-genome
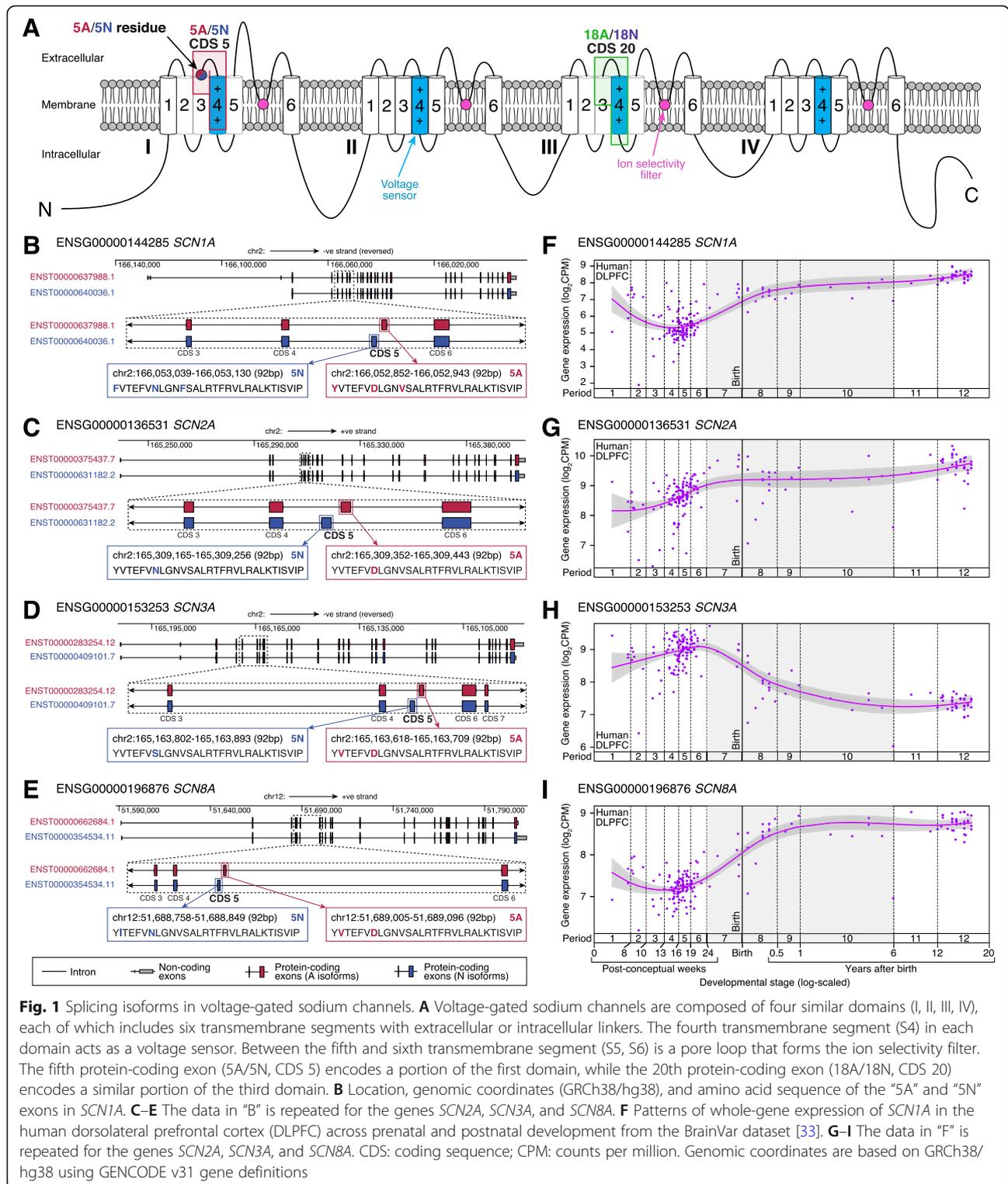
Fig. 1 Splicing isoforms in voltage-gated sodium channels. **A** Voltage-gated sodium channels are composed of four similar domains (I, II, III, IV), each of which includes six transmembrane segments with extracellular or intracellular linkers. The fourth transmembrane segment (S4) in each domain acts as a voltage sensor. Between the fifth and sixth transmembrane segment (S5, S6) is a pore loop that forms the ion selectivity filter. The fifth protein-coding exon (5A/5N, CDS 5) encodes a portion of the first domain, while the 20th protein-coding exon (18A/18N, CDS 20) encodes a similar portion of the third domain. **B** Location, genomic coordinates (GRCh38/hg38), and amino acid sequence of the "5A" and "5N" exons in *SCN1A*. **C–E** The data in "B" is repeated for the genes *SCN2A*, *SCN3A*, and *SCN8A*. **F** Patterns of whole-gene expression of *SCN1A* in the human dorsolateral prefrontal cortex (DLPFC) across prenatal and postnatal development from the BrainVar dataset [33]. **G–I** The data in "F" is repeated for the genes *SCN2A*, *SCN3A*, and *SCN8A*. CDS: coding sequence; CPM: counts per million. Genomic coordinates are based on GRCh38/hg38 using GENCODE v31 gene definitions

sequencing data that were used to derive per sample genotypes, as described previously [33]. To assess exon expression across brain regions, we assessed bulk-tissue RNA-seq data from 607 *postmortem* neurologically normal samples from 41 individual brains across 11 cortical regions, hippocampus, amygdala, mediodorsal nucleus of the thalamus, striatum, and cerebellar cortex from the BrainSpan cohort (Additional File 2: Table S1) [12, 34]. The deidentified BrainSpan samples ranged from 8 post-conception weeks and 40 years of age with 23 males and

18 females. To assess corresponding patterns of exon expression in mouse cortex across development, we assessed 58 cortical samples with bulk tissue RNA-seq data in wildtype C57BL/6 J (JAX: 000664) mice (Additional File 2: Table S1). Thirty-four of these were generated as controls for ongoing experiments. These animals were housed with littermates in a vivarium with a 12-h light, 12-h dark cycle. Embryonic day 0.5 was defined as noon on the day the vaginal plug was detected. Data for the remaining 24 mice were downloaded from GEO [35].

Exon expression
To assess exon expression in the human cortex, the 100 bp paired-read RNA-seq data from BrainVar were aligned to the GRCh38.p12 human genome using STAR aligner [36], and exon-level read counts for GENCODE v31 human gene definitions were calculated with DEXSeq [37] and normalized to counts per million (CPM) [38]. Despite the similar amino acid sequence, the nucleotide sequence of 5A and 5N is sufficiently differentiated across the four genes that 100 bp reads align unambiguously to one location in the genome [39]. Reads were detected in 5A and 5N for all samples, across all four genes, with the exception of SCN1A for which 31 of 176 samples (17.6%) had no detectable 5N reads (Fig. 2A). Along with quantifying the expression of 5N and 5A (Fig. 2), we also assessed expression for the surrounding constitutive exons, as a control. The Brain-Span data were analyzed using the same methods. For the mouse cortical data, the same analysis methods were used but with alternative references, specifically the GRCm38/mm10 genome and GENCODE vM25 gene definitions. A similar approach was used to assess the utilization of 18A and 18N in SCN8A/Scn8a.

Intron splicing
We applied a complementary approach to detecting 5A and 5N exon usage by assessing intron splicing via reads that map across exon-exon junctions in the same Brain-Var samples. Reads were aligned with OLego aligner [40] using the same genome build and gene definitions as for exon expression. Clusters of differential intron splicing were identified with Leafcutter [41] and differences across development were detected by comparing 112 prenatal samples to 60 postnatal samples, excluding 4 samples in the transitional late fetal period [33]. No cluster was detected for 5A/5N in SCN1A, preventing assessment across development, but 5A/5N clusters were identified and assessed for the other three genes and for 18A/18N in SCN8A (Figs. 3 and 5).

Quantitative trait locus (QTL) analysis
Common variants with a minor allele frequency ≥ 5% in both prenatal (N = 112) and postnatal (N = 60) samples

and Hardy Weinberg equilibrium p value $\geq 1 \times 10^{-12}$ were identified previously [33]. Variants within one million basepairs of each sodium channel gene were extracted and integrated with the Leafcutter clusters, along with the first five principal components calculated from common variants identified in whole-genome sequencing data from these samples and 3804 parents from the Simons Simplex Collection [33, 42] to predict splicing QTLs with FastQTL [43]. This analysis was performed on all samples, prenatal-only samples, and postnatal-only samples, with false discovery rate (FDR) estimated from the results of each analysis using the Benjamini-Hochberg procedure [44]. To assess the correlation of 5N expression for the SNP rs3812718, genotypes were extracted for chr2:166,053,034 C>T (GRCh38) and compared with 5N expression calculated by DEXSeq, as described above.

Statistical analysis
The 5A:5N expression ratio was calculated from normalized exon expression values (CPM). Linear regression was used to assess whether this ratio varied across development by comparing the log-transformed 5A:5N ratio to log-transformed post-conceptual days (Fig. 2). The difference in 5A:5N ratio was also assessed between the mid-late fetal samples (N = 112) and childhood/adolescent/young adult samples (N = 35) with a two-tailed Wilcoxon test. To compare intron splicing between prenatal and postnatal samples, we used the p-values estimated with a Dirichlet-multinomial generalized linear model, as implemented in Leafcutter [41]. The same approach was used to calculate 18A:18N ratios for SCN8A.

Results
Expression of voltage-gated sodium channels in the human cortex
Gene expression varies dramatically across development for many genes, especially during the late-fetal transition, during which half the genes expressed in the brain undergo a concerted increase or decrease in expression [12, 33, 34, 45]. To assess gene-level developmental trajectories, we analyzed bulk-tissue RNA-seq in 176 *post-mortem* samples from the BrainVar cohort (104 male, 72 female, spanning 6 post-conceptual weeks to 20 years after birth) from the dorsolateral prefrontal cortex (DLPFC, N = 167 older than 10 post-conception weeks) or frontal cerebral wall (N = 9 younger than 10 post-conception weeks) [33]. The gene-level expression profile of all four voltage-gated sodium channels changes during this late-fetal transition (Fig. 1F–I), with SCN1A, SCN2A, and SCN8A expression rising from mid-fetal development through infancy to early childhood, while SCN3A expression falls.
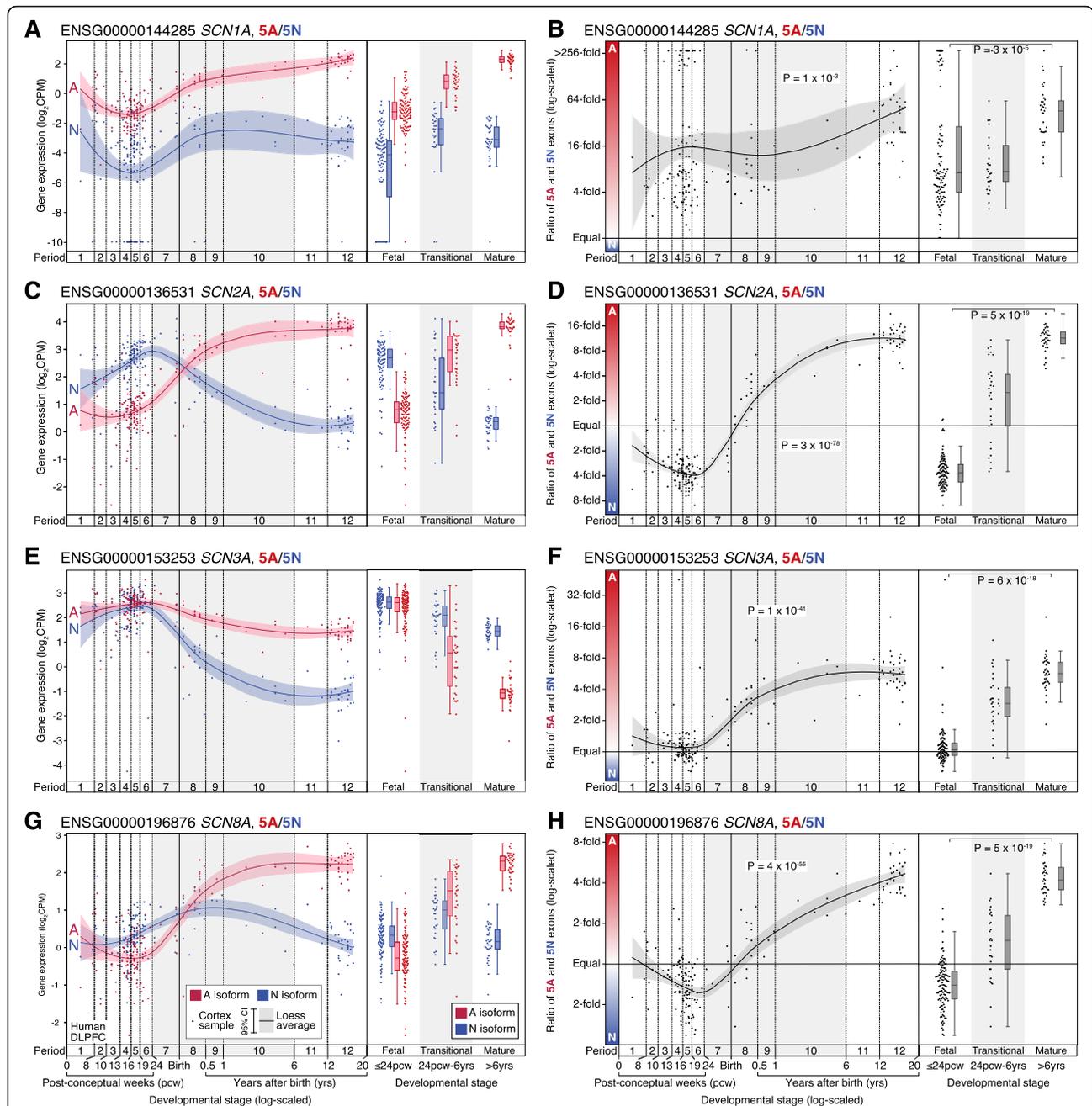
Fig. 2 Expression of 5A and 5N in the human cortex across development. **A** The expression of 5A (red) and 5N (blue) in *SCN1A* is shown for 176 BrainVar human cortex (DLPFC) samples across development (points). On the left, the colored line shows the Loess smoothed average and 95% confidence interval (shaded region). On the right, boxplots show the median and interquartile range for the same data, binned into fetal, transitional, and mature developmental stages. **B** The ratio of 5A and 5N expression from panel **A** is shown across development (left) and in three developmental stages (right). **C–H** Panels **A** and **B** are repeated for the genes *SCN2A*, *SCN3A*, *SCN8A*. For comparison, the 5A/5N ratio is shown on the same *y*-axis in Additional file 1: Fig. S3, and equivalent plots for CDS four and six are shown in Additional file 1: Fig. S4. CPM: Counts per million; DLPFC: Dorsolateral prefrontal cortex. Statistical tests: **B**, **D**, **F**, **H** Left panel, linear regression of $\log_2$(5A:5N ratio) and $\log_2$(post-conceptual days). Right panel, two-tailed Wilcoxon test of $\log_2$(5A:5N ratio) values between fetal and mature groups

Developmental trajectories of 5A and 5N expression in the human cortex

The majority of protein-coding exons follow the expression trajectory of their parent gene across development (Additional file 1: Fig. S2); however, all four sodium channels show dynamic changes in the utilization of 5A/ 5N (Fig. 2, Additional file 1: Fig. S3). This is especially marked for *SCN2A* and *SCN8A*, where 5N is expressed
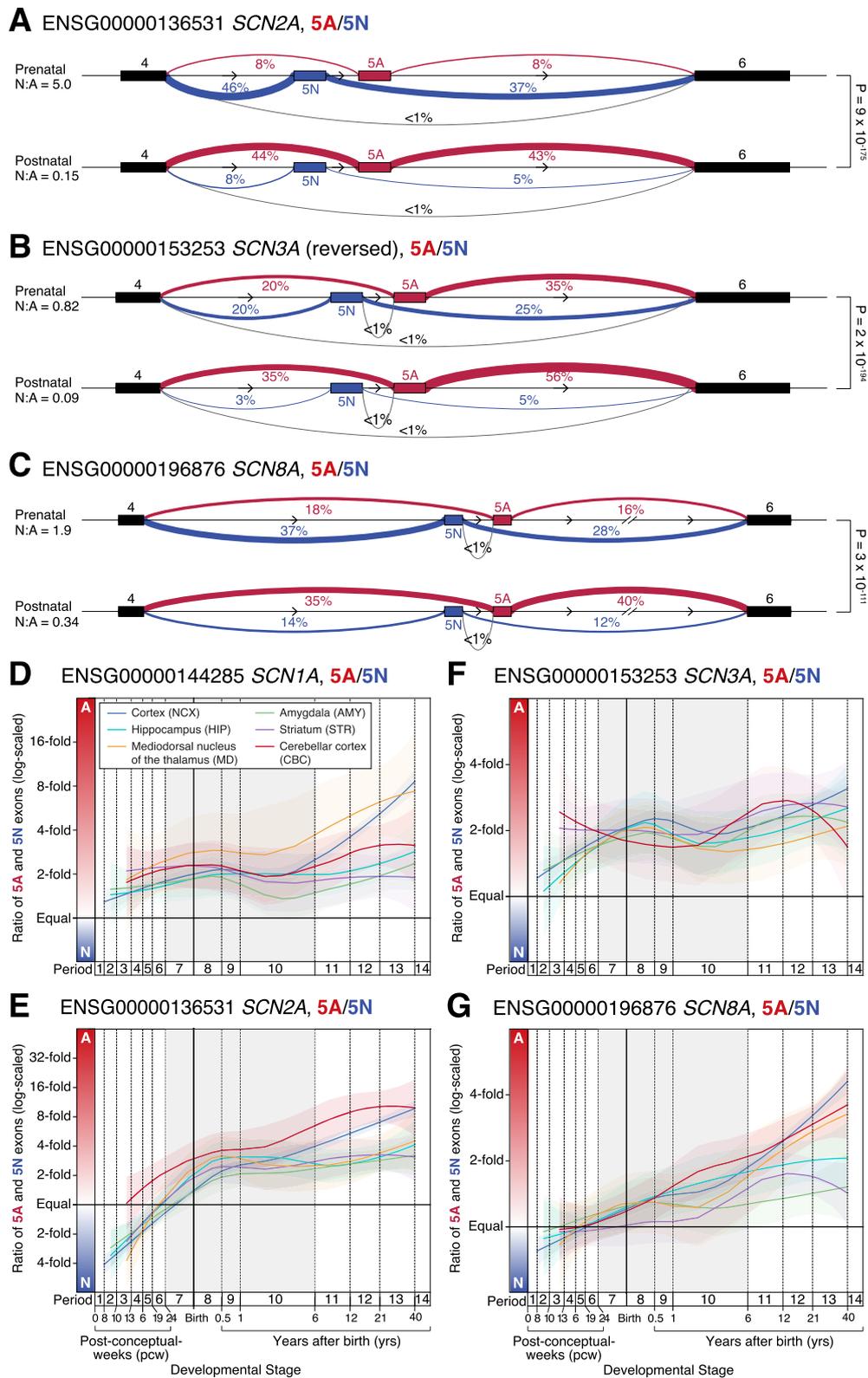
Fig. 3 (See legend on next page.)

(See figure on previous page.)

Fig. 3 Orthogonal analysis of voltage-gated sodium channel gene splicing in the developing human brain. **A** Sashimi plot of splicing in prenatal (top, N = 112 samples) and postnatal (bottom, N = 60 samples) DLPFC for *SCN2A*. Linewidth reflects the proportion of split reads observed for each intron compared to all split reads between CDS 4 and CDS 6, this value is also shown as a percentage. Introns related to 5A inclusion are shown in red, those related to 5N inclusion are shown in blue, and others are in grey. **B, C** Equivalent plots for *SCN3A* (a negative-strand gene with the orientation reversed to facilitate comparison to the other two genes) and *SCN8A*. **D** The ratio of 5A and 5N expression is shown across development for *SCN1A* in six human brain regions. For each region, the colored line shows the Loess smoothed average and 95% confidence interval (shaded region). Equivalent data across 11 cortical regions are shown in Additional file 1: Fig. S6. **E**–**G** This analysis is repeated for *SCN2A*, *SCN3A*, and *SCN8A*. Statistical tests: **A**–**C** *P* values compare the prenatal and postnatal cluster using a Dirichlet-multinomial generalized linear model, as implemented in Leafcutter [41]

at a higher level than 5A in the mid-fetal brain but this reverses soon after birth. Plotting the 5A:5N ratio allows exon utilization to be assessed independent of changes in gene expression (Fig. 2). All four genes show changes in the 5A:5N ratio across development, with a modest change for *SCN1A* (7.1 fetal to 45.7 childhood/adolescent; $p = 3 \times 10^{-5}$, two-sided Wilcoxon test, Fig. 2B) and dramatic changes for *SCN2A* (0.27 to 11.4; $p = 5 \times 10^{-19}$, Fig. 2D), *SCN3A* (1.0 to 5.7; $p = 6 \times 10^{-18}$, Fig. 2F), and *SCN8A* (0.7 to 4.2; $p = 5 \times 10^{-19}$, Fig. 2H). As a control, we applied this approach to assess the ratio of the neighboring protein-coding exons: coding sequence (CDS) 4 and CDS 6. We observed no developmental shift in the 4:6 ratio for *SCN1A*, *SCN2A*, and *SCN3A*; however, the exon 4:6 ratio is marginally higher than expected in the prenatal period for *SCN8A* (0.82 vs. 0.66; 9×10^{-10}, Additional file 1: Fig. S4). This developmental variation in *SCN8A* is not observed for the surrounding protein-coding exons and reflects a modest increase in CDS 4 expression in the prenatal period, based on the expected expression given the exon length (Additional file 1: Fig. S2, Additional file 1: S5).

Intron splicing around 5A and 5N in the human cortex

To verify that mutually exclusive use of 5A and 5N underlies the observed exon expression changes (Fig. 2), we considered RNA-seq reads that spanned exon-exon junctions to quantify intron splicing in BrainVar. Clusters of differential intron splicing corresponding to 5A/5N usage were identified by Leafcutter for *SCN2A*, *SCN3A*, and *SCN8A* (Fig. 3A–C), but not *SCN1A*, likely due to the consistently low expression of N isoforms (Fig. 2). The splicing patterns for *SCN2A*, *SCN3A*, and *SCN8A* are consistent with the observed exon expression changes (Figs. 2 and 3) and at least 99% of reads are consistent with mutually exclusive 5A/5N utilization.

Developmental trajectories of 5A and 5N expression across human brain regions

To assess 5A and 5N expression across multiple brain regions we repeated the exon expression analysis in 607 samples from 41 individual *postmortem* human brains in the BrainSpan cohort [12, 34]. A similar trajectory of 5A:
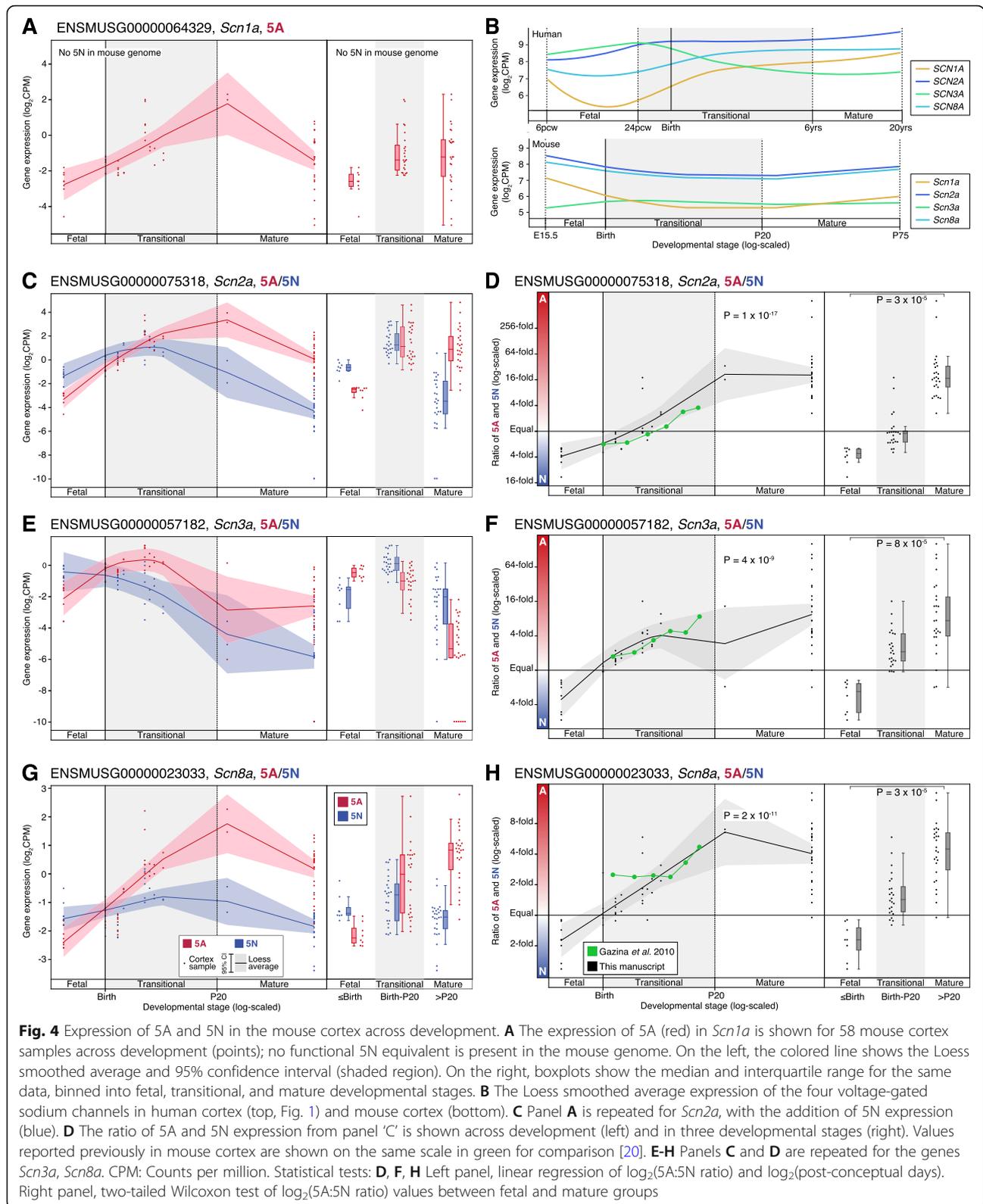
5N utilization was observed for all four sodium channels across the cortex, hippocampus, amygdala, striatum, mediodorsal nucleus of the thalamus, and cerebellar cortex (Fig. 3D–G) and across eleven cortical regions (Additional file 1: Fig. S6).

Developmental trajectories of 5A and 5N expression in the mouse cortex

We repeated the analysis of sodium channel 5A/5N expression using bulk-tissue RNA-seq data from the mouse cortex across development (N = 58; E15.5 to P75). Our data are consistent with the 5A:5N ratios described previously (Fig. 4), however, by assessing a wider developmental period we observe more substantial differences at the extremes of development: *Scn2a* (0.3 fetal to 17.3 mature; $p = 3 \times 10^{-5}$, two-sided Wilcoxon test, Fig. 4C), *Scn3a* (0.4 to 7.4; $p = 8 \times 10^{-5}$, Fig. 4E), and *Scn8a* (0.6 to 4.5; $p = 3 \times 10^{-5}$, Fig. 4G). Mice lack a functional 5N exon in *Scn1a*.

No evidence of common polymorphisms regulating 5A or 5N utilization

A common polymorphism (rs3812718, GRCh38 chr2: 166,053,034 C>T, IVS5N+5G>A) has previously been associated with epilepsy, seizures, and response to antiepileptics [21, 22, 29, 46, 47], though this variant did not reach genome-wide significance in a mega-analysis of epilepsy [48]. Prior analyses of expression in the adult human temporal cortex showed evidence that the homozygous variant allele (TT in DNA, AA in cDNA) was associated with reduced utilization of 5N in *SCN1A* [21, 49]. We do not observe evidence for such a relationship in the prenatal or postnatal prefrontal cortex (Additional file 1: Fig. S7) and this polymorphism is not identified as a splicing quantitative trait locus (sQTL) in GTEx (50). Furthermore, this variant is not predicted to alter splicing behavior using the SpliceAI algorithm [50]. We did not identify rs3812718 as an expression quantitative trait locus (eQTL) in the BrainVar cohort and do not see evidence of a relationship to *SCN1A* gene-wide expression (Additional file 1: Fig. S7), however, in GTEx, the TT genotype is associated with increased *SCN1A* expression in the adult human basal ganglia ($p = 1 \times 10^{-10}$) [51].

Fig. 4 Expression of 5A and 5N in the mouse cortex across development. **A** The expression of 5A (red) in *Scn1a* is shown for 58 mouse cortex samples across development (points); no functional 5N equivalent is present in the mouse genome. On the left, the colored line shows the Loess smoothed average and 95% confidence interval (shaded region). On the right, boxplots show the median and interquartile range for the same data, binned into fetal, transitional, and mature developmental stages. **B** The Loess smoothed average expression of the four voltage-gated sodium channels in human cortex (top, Fig. 1) and mouse cortex (bottom). **C** Panel **A** is repeated for *Scn2a*, with the addition of 5N expression (blue). **D** The ratio of 5A and 5N expression from panel 'C' is shown across development (left) and in three developmental stages (right). Values reported previously in mouse cortex are shown on the same scale in green for comparison [20]. **E-H** Panels **C** and **D** are repeated for the genes *Scn3a, Scn8a*. CPM: Counts per million. Statistical tests: **D**, **F**, **H** Left panel, linear regression of $\log_2$(5A:5N ratio) and $\log_2$(post-conceptual days). Right panel, two-tailed Wilcoxon test of $\log_2$(5A:5N ratio) values between fetal and mature groups

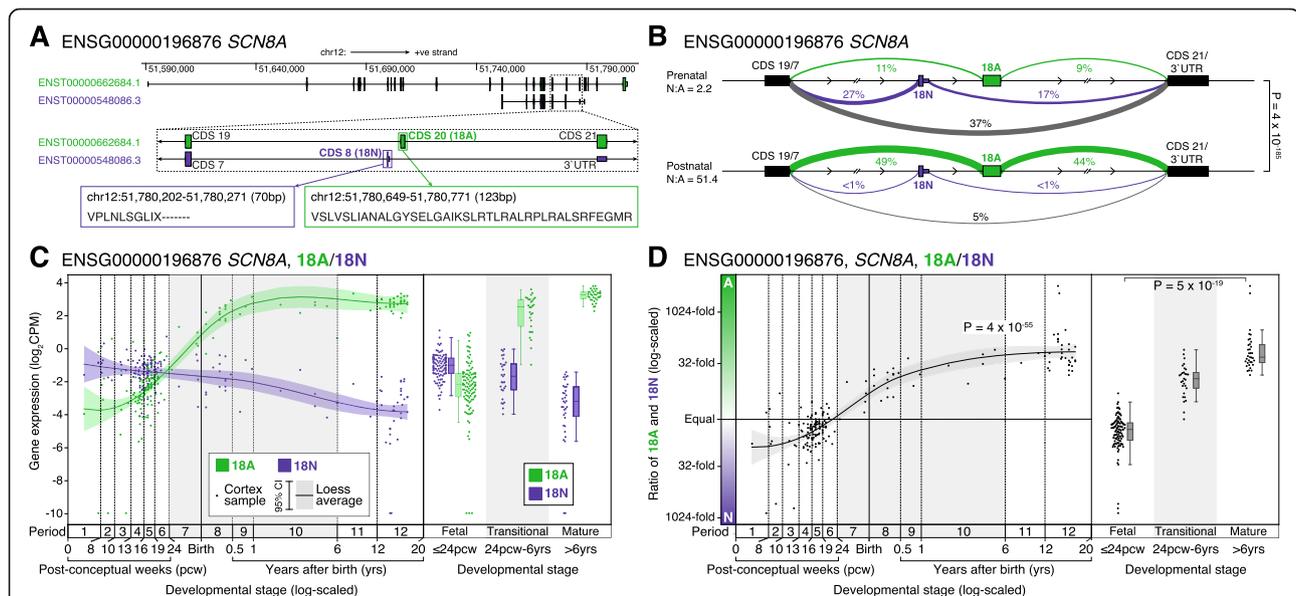## Developmental trajectories of 18A and 18N expression in *SCN8A*

We next considered the developmental timing of the transition between 18A and 18N in *SCN8A* (Figs. 1A and 5A). Intron splicing shows a robust difference between prenatal and postnatal human dorsolateral prefrontal cortex ($P = 4 \times 10^{-185}$, Fig. 5B), with the prenatal period characterized by high frequencies of transcripts excluding 18A, either including 18N or skipping both 18N and 18A, while in the postnatal cortex 18A is included in 93% of reads. Considering exon expression (Fig. 5C, D), the expression of 18A increases markedly over development and this is distinct from other protein-coding exons for *SCN8A* (Additional file 1: Fig. S2). Consistent with prior analyses of the human brain [23], the 18A/18N transition begins around 13 postconceptual weeks and continues till 6 months of age, with both timepoints being earlier than the equivalents for 5A/5N in *SCN8A* and the other genes.

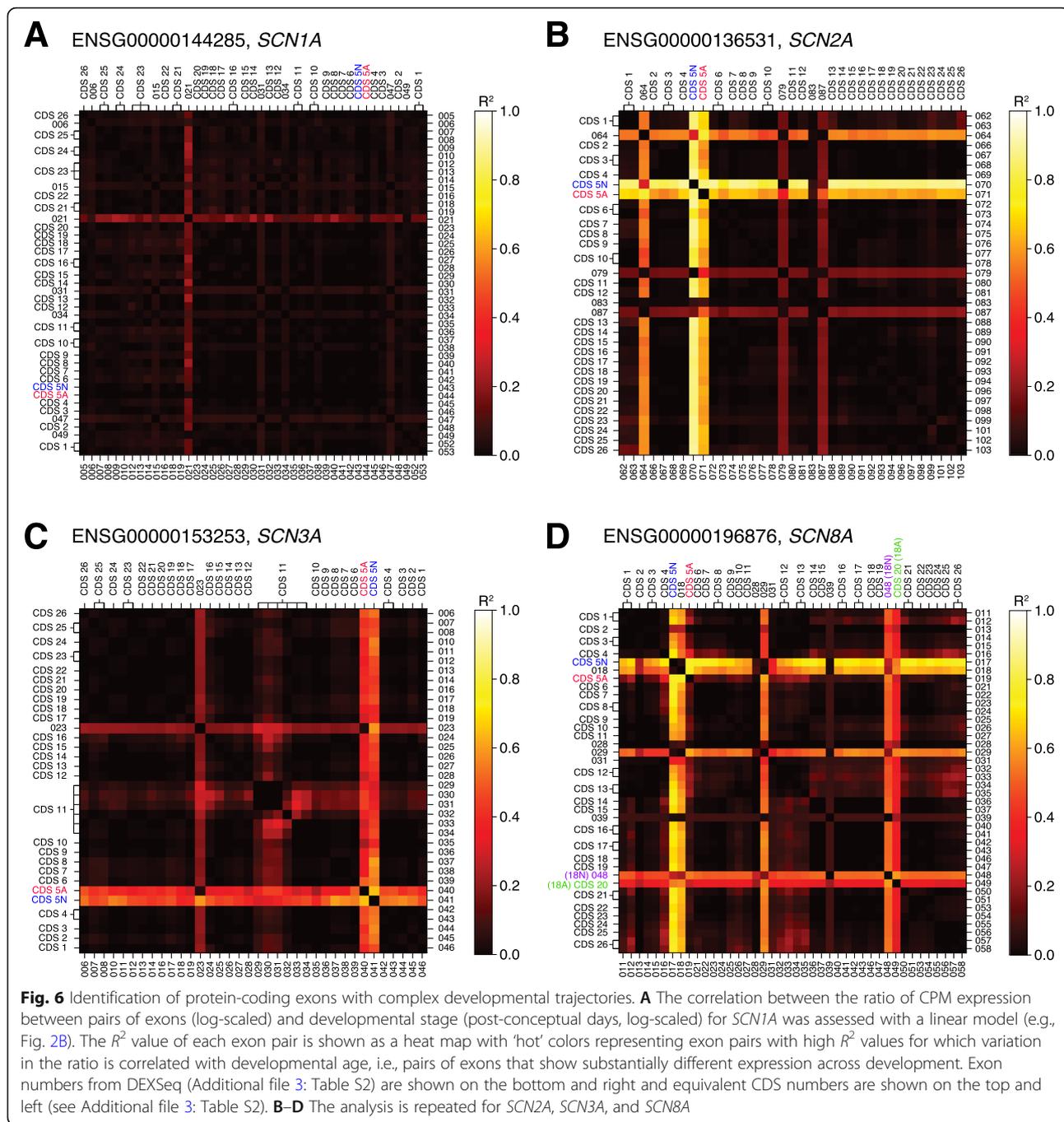## Other annotated protein-coding exons with distinct developmental trajectories

To assess whether other protein-coding exons undergo distinct developmental transitions (Additional file 1: Fig.

S2), we calculated the ratios of all pairs of protein-coding exons within each of the four sodium channel genes and assessed whether the ratio was correlated with developmental stage using linear regression. This is the same calculation used to quantify the 5A/5N and 18A/18N transitions (Figs. 2 and 5D) and distinguishes exons with expression profiles that differ from the rest of the gene (e.g., 5A in *SCN2A*), rather than simply being expressed at reduced levels, suggesting alternative regulatory processes (Additional file 1: Fig. S2). Visualizing the R^2 values of these correlations provides a simple method to identify such distinct developmental trajectories (Fig. 6). Aside from 5A/5N and, in *SCN8A*, 18A/18N, no protein-coding exons common to most isoforms (consistent CDS in Additional file 1: Fig. S2) show differential expression across development, but a few weakly expressed protein-coding exons specific to a small number of isoforms do (variable CDS in Additional file 1: Fig. S2) (Fig. 6).

GENCODE defines seven variable CDS exons for *SCN1A* (DEXSeq divisions: 006, 015, 021, 031, 034, 047, 049; Additional file 3: Table S2, Fig. 6A). Of these, only 021 shows a distinct developmental trajectory (Fig. 6A), with reduced postnatal expression relative to other

Fig. 5 Developmental trajectories of CDS 20 (18A/18N) in human cortex in *SCN8A*. **A** Location, genomic coordinates (GRCh38/hg38), and amino acid sequence of the 18A and 18N exons in *SCN8A*. **B** Sashimi plot of intron splicing in prenatal (top, N = 112 samples) and postnatal (bottom, N = 60 samples) dorsolateral prefrontal cortex. Linewidth reflects the proportion of split reads observed for each intron compared to all split reads between the exon before and after, this value is also shown as a percentage. Introns related to 18A exon inclusion are shown in green, those related to 18N exon inclusion are shown in purple, and others are in grey. **C** Expression of the 18A (green) and 18N (purple) for 176 BrainVar human dorsolateral prefrontal cortex samples across development (points). On the left, the colored line shows the Loess smoothed average with the shaded area showing the 95% confidence interval. On the right, boxplots show the median and interquartile range for the same data, binned into fetal, transitional, and mature developmental stages. **D** The 18A:18N ratio is shown for each sample from panel **C** across development (left) and binned into three groups (right). CPM: Counts per million; Statistical analyses: **B** Dirichlet-multinomial generalized linear model, as implemented in Leafcutter [41]. **D** Left panel, linear regression of $\log_2$(18A:18N ratio) and $\log_2$(post-conceptual days). Right panel, two-tailed Wilcoxon test of $\log_2$(18A:18N ratio) values between fetal and mature groups

Fig. 6 Identification of protein-coding exons with complex developmental trajectories. **A** The correlation between the ratio of CPM expression between pairs of exons (log-scaled) and developmental stage (post-conceptual days, log-scaled) for *SCN1A* was assessed with a linear model (e.g., Fig. 2B). The R^2 value of each exon pair is shown as a heat map with 'hot' colors representing exon pairs with high R^2 values for which variation in the ratio is correlated with developmental age, i.e., pairs of exons that show substantially different expression across development. Exon numbers from DEXSeq (Additional file 3: Table S2) are shown on the bottom and right and equivalent CDS numbers are shown on the top and left (see Additional file 3: Table S2). **B–D** The analysis is repeated for *SCN2A*, *SCN3A*, and *SCN8A*

SCN1A exons (Additional file 1: Fig. S2). This result is verified by the intron splicing data ($p = 6 \times 10^{-91}$, Leafcutter).

In *SCN2A*, the 5A/5N trajectories stand out clearly (Fig. 6B). There are four variable CDS exons (DEXSeq divisions: 064, 079, 083, 087; Additional file 3: Table S2, Fig. 6B), three of which have distinct developmental trajectories (Fig. 6B, Additional file 1: Fig. S4): 064 (Additional file 1: Fig. S2, $P = 2 \times 10^{-12}$, Leafcutter), 079 (Additional file 1: Fig. S2, $P = 7 \times 10^{-33}$, Leafcutter), 087

(Additional file 1: Fig. S2, $P = 2 \times 10^{-20}$, Leafcutter). The single variable CDS exon in *SCN3A*, 023 (Additional file 3: Table S2, Fig. 6C), varies across development (Additional file 1: Fig. S2, $P = 3 \times 10^{-80}$, Leafcutter). Finally, aside from 18N, there are five variable CDS exons in *SCN8A* (DEXSeq divisions: 018, 028, 029, 031, 039; Additional file 3: Table S2, Fig. 6D) of which 018 and 029 vary across development (Fig. 6D), but neither of these is validated by Leafcutter.

Discussion

Using transcriptomic data from 176 human prefrontal cortex samples and 607 samples across 16 brain regions, we characterized the developmental patterns for protein-coding exons in *SCN1A*, *SCN2A*, *SCN3A*, and *SCN8A* (Fig. 6, Additional file 1: Fig. S4). We observed a coordinated increase in the 5A:5N ratio between 24 post-conceptual weeks (2nd trimester) and six years of age across brain regions, which is synchronized with widespread transcriptomic changes in the brain during the late-fetal transition [33, 34]. This is preceded by a similar increase in the 18A:18N ratio in *SCN8A* from 13 post-conceptual weeks to 6 months of age, which is regulated by RBFOX1 [15, 23, 31]. By analyzing a wider developmental window than prior analyses [20, 21, 23, 49], we observed more dynamic changes and larger disparities in exon expression. These splicing changes modify channel function [24, 27], neuronal behavior [28], and clinical phenotypes [21, 22, 29] and interact with specific disorder-associated variants [24].

Recent advances have shown that differential splicing patterns can be effective therapeutic targets in humans, for example through intrathecal antisense oligonucleotides (ASOs) [52, 53], and rapid progress is being made with ASOs to modify gene-wide expression in rodent models of some voltage-gated sodium channel disorders [54–56]. Manipulating the expression of specific exons in these genes may represent a complementary therapeutic strategy; we consider several therapeutic scenarios.

First, for individuals with disorder-associated genetic variants within the 30 amino acids encoded by either 5A or 5N, expressing the other copy of 5A/5N could skip the variant. Theoretically, this approach could benefit individuals with both loss-of-function (protein-truncating variants, missense, splice site) and severe gain-of-function (missense) variants and at least eight cases of epileptic encephalopathy have been identified with variants in 5A of *SCN2A* or *SCN8A* [13, 19, 57, 58]. Epilepsy resulting from many of these variants is poorly managed with antiepileptic drugs [13], which either block sodium channels with limited isoform specificity or target other mechanisms (e.g., other ion channels). Whether such a strategy offers benefits over simply reducing overall channel expression [54, 56] remains to be seen, however, there may be additional effects of decreasing expression of both the normal and variant-containing alleles. Such conditions could mimic cases of *SCN2A* haploinsufficiency, associated with autism spectrum disorder and intellectual disability [13, 58, 59]. Furthermore, some children with *SCN2A* haploinsufficiency experience seizures, and recent work suggests that lowering *SCN2A* expression levels below 50% may increase the prevalence of such seizure conditions [60–62]. Thus, for this subset of patients, splice-altering ASOs may provide a wider therapeutic window than ASOs that reduce gene expression. The success of such a therapy would depend upon the proportion of transcripts expressing the alternate 5th exon and the ability of this exon to functionally replace the original 5th exon.

Second, in *SCN8A*, gain-of-function variants lead to epileptic encephalopathy. Reducing the levels of the encoded $Na_V1.6$ channel should improve symptoms, as demonstrated by an ASO that degrades *SCN8A* mRNA in mice [54]. Interventions that promote exon skipping of 18A or exon switching from 18A to 18N would prevent translation of functional $Na_V1.6$ channels, leading to a similar effect. All interventions aimed at reducing *SCN8A* levels would require very careful dosing since *SCN8A* haploinsufficiency is strongly associated with intellectual disability [63].

Third, splice isoforms can also affect the biophysical effects of variants outside of 5A and 5N. Two variants associated with benign infantile seizures—M252V and L1563V—exhibit biophysical changes only when expressed on 5N isoform [19, 27]. Since benign infantile seizures resolve spontaneously these are not candidates for novel, potentially risky, therapies, however, they demonstrate the existence of variants with isoform-specific impacts on the biophysical properties of the channel. Three recently characterized epileptic encephalopathy-associated variants in *SCN2A*—T236S, E999K, and S1336Y—all exhibit more pronounced alterations in their electrophysiological properties in 5N $Na_V1.2$ isoforms compared to 5A isoforms [24]. For individuals with these and equivalent variants, tilting expression towards the 5A isoform could provide some symptomatic improvement, especially during infancy. Conversely, if variants exist with more pronounced effects in the 5A isoform, then encouraging 5N expression may be beneficial. Critically, such an approach relies on detailed electrophysiological characterization of specific variants, both in heterologous expression systems and in neuronal cell lines or rodent models, as data obtained for individual variants in expression systems can vary based on recording conditions and co-expression of sodium channel auxiliary subunits [24, 27]. At present, the burden of characterization limits the translational potential of such allele-specific interventions compared with gene-specific approaches [54–56]; however, technological advances or large-scale characterization efforts could provide future opportunities.

Finally, modifying 5A/5N splicing might aid seizure control in older children and adults. At this age, the 5A isoform is predominantly utilized in both *SCN2A* or *SCN8A*, which are critical for regulating the excitability of glutamatergic neurons [7, 11, 60, 61]. Reverting expression to the fetal/neonatal state by encouraging 5N

utilization could reduce the excitability of cortical gluta-matergic neurons, potentially limiting seizures [60]. For ASOs, the repeated intrathecal administration would limit such an approach to the most severe cases of epi-lepsy, however, small molecules can also modify splicing behavior [64]. It remains to be seen whether this ap-proach could offer therapeutic benefits above and be-yond existing antiepileptic drugs.

Our analysis was limited by the use of short-read tran-scriptomic data, leading us to focus on quantifying exon-level expression (Fig. 2) and splice junction usage (Fig. 3), rather than relying on estimates of isoform utilization (Additional file 1: Fig. S1). We also elected to focus on protein-coding transcripts and exons defined by GENCODE (v31) rather than attempting de novo transcriptome assembly. Emerging long-read transcrip-tomic technology may substantially expand estimates of isoform and exon diversity but these technologies have not been applied to the developing human brain at scale [65, 66]. We also note that transcriptomic data is only partially predictive of protein levels and other factors, in-cluding channel transport and degradation, may influ-ence the impact of isoforms on neuronal function. Comparing results from the human and mouse cortex (Figs. 2 and 4), more substantial differences in gene and exon expression may be observed at earlier embryonic times in the mouse or with larger sample sizes. In addition, the use of bulk-tissue transcriptomic data limits our ability to assess how individual cell types or cell states contribute to the observed isoform trajectories. Technological and methodological advances may provide insights at cell-level resolution in the future [67].

Conclusions

Dramatic differences in exon usage of *SCN1A*, *SCN2A*, *SCN3A*, and *SCN8A* observed in rodent brains also occur in the developing human brain, beginning in fetal development and continuing through early childhood. These changes in splicing affect the biophysical proper-ties of the encoded channels and are likely to contribute to differences in phenotype observed between indivi-duals with different variants and across development. Manipulation of these splicing patterns may have thera-peutic applications.

Supplementary Information

The online version contains supplementary material available at https://doi.org/10.1186/s13073-021-00949-0.

Additional file 1:. Supplementary Figures; Supplementary Figures 1 to 7 accompanying the main text.

Additional file 2:. Table S1 – Sample information; Metadata on human and mouse samples used in this study, including age, sex, tissue, and sequencing conditions.

Additional file 3:. Table S2 – Exon information; Details of the voltage-gated sodium channel gene exons featured in this study.

Additional file 4:. Supplementary materials

Availability of data and materials

The BrainVar data are available through the PsychENCODE Knowledge Portal: syn21557948 on Synapse.org (https://www.synapse.org/#!Synapse:syn4921369) [33]. The BrainSpan data are also available through the PsychENCODE Knowledge Portal: syn6136125 on Synapse.org (https://www.synapse.org/#!Synapse:syn6136125) [12, 34]. Scripts used in this manuscript can be found on Github [68].

Declarations

Ethics approval and consent to participate

This study was conducted using de-identified human data therefore IRB review was not required. IRB procedures for the data generation have been described previously [12, 33, 34]. For the mouse data, all procedures and animal care were approved by the UCSF Institutional Animal Care Use Committee (IACUC, AN180174-03) and performed in accordance with the University of California San Francisco Laboratory Animal Research Center (LARC) guidelines. The research performed conformed to the principles of the Helsinki Declaration.

Consent for publication

This study was conducted using de-identified human data available for general research use [12, 33, 34].

Competing interests

J.L.R.R. is cofounder, stockholder, and currently on the scientific board of *Neurona*, a company studying the potential therapeutic use of interneuron transplantation. S.J.S. receives research funding from *BioMarin Pharmaceutical Inc.* The remaining authors declare that they have no competing interests.

Liang *et al. Genome Medicine*   (2021) 13:135

Page 13 of 14

Author details

[1]Department of Psychiatry and Behavioral Sciences, UCSF Weill Institute for Neurosciences, University of California, San Francisco, San Francisco, CA 94158, USA. [2]Department of Neuroscience and Kavli Institute for Neuroscience, Yale School of Medicine, New Haven, CT 06510, USA. [3]Department of Neurology, UCSF Weill Institute for Neurosciences, University of California, San Francisco, San Francisco, CA 94158, USA. [4]School of Biosystem and Biomedical Science, College of Health Science, Korea University, Seoul 02841, Republic of Korea. [5]Laboratory of Genetics, University of Wisconsin-Madison, Madison, WI 53706, USA. [6]Program in Cellular Neuroscience, Neurodegeneration, and Repair and Yale Child Study Center, Yale School of Medicine, New Haven, CT 06510, USA. [7]Department of Psychiatry, Yale University School of Medicine, New Haven, CT 06520, USA. [8]Department of Genetics, Yale University School of Medicine, New Haven, CT 06520, USA. [9]Department of Comparative Medicine, Program in Integrative Cell Signaling and Neurobiology of Metabolism, Yale School of Medicine, New Haven, CT 06510, USA. [10]Institute for Human Genetics, University of California, San Francisco, San Francisco, CA 94158, USA. [11]Bakar Computational Health Sciences Institute, University of California, San Francisco, San Francisco, CA 94158, USA.

References

1. Heyne HO, Singh T, Stamberger H, Abou Jamra R, Caglayan H, Craiu D, et al. De novo variants in neurodevelopmental disorders with epilepsy. Nat Genet [Internet]. 2018;1. Available from: http://www.nature.com/articles/s41588-018-0143-7
2. Satterstrom FK, Kosmicki JA, Wang J, Breen MS, De Rubeis S, An J-Y, et al. Large-Scale Exome Sequencing Study Implicates Both Developmental and Functional Changes in the Neurobiology of Autism. Cell. 2020 Jan;
3. Kaplanis J, Samocha KE, Wiel L, Zhang Z, Arvai KJ, Eberhardt RY, et al. Integrating healthcare and research genetic data empowers the discovery of 49 novel developmental disorders. bioRxiv [Internet]. 2019 Jan 1;797787. Available from: http://biorxiv.org/content/early/2019/10/16/797787.abstract
4. Catterall WAWA, Marban E, Catterall WAWA, Cestèle S, Catterall WAWA, Wood JN, et al. Voltage-gated sodium channels. J Physiol [Internet]. 2001; 1(1):17–21 Available from: http://www.pubmedcentral.nih.gov/articlerender.fcgi?artid=3885250&tool=pmcentrez&rendertype=abstract%5Cn, http://www.pubmedcentral.nih.gov/articlerender.fcgi?artid=3424717&tool=pmcentrez&rendertype=abstract%5Cn, http://onlinelibrary.wiley.com/doi/10.1111/j.14.
5. Bender KJ, Trussell LO. The physiology of the axon initial segment. Annu Rev Neurosci. 2012;35(1):249–65. https://doi.org/10.1146/annurev-neuro-062111-150339.
6. Kole MHP, Stuart GJ. Signal processing in the axon initial segment. Neuron [Internet] 2012 Jan;73(2):235–47. Available from: https://doi.org/10.1016/j.neuron.2012.01.007
7. Spratt PWE, Ben-Shalom R, Keeshen CM, Burke KJJ, Clarkson RL, Sanders SJ, et al. The Autism-Associated Gene Scn2a Contributes to Dendritic Excitability and Synaptic Function in the Prefrontal Cortex. Neuron. 2019 Aug;103(4):673–685.e5.
8. Hu W, Tian C, Li T, Yang M, Hou H, Shu Y. Distinct contributions of Na(v)1.6 and Na(v)1.2 in action potential initiation and backpropagation. Nat Neurosci [Internet]. 2009;12(8):996–1002. Available from: http://www.ncbi.nlm.nih.gov/pubmed/19633666
9. Smith RS, Kenny CJ, Ganesh V, Jang A, Borges-Monroy R, Partlow JN, et al. Sodium Channel SCN3A (Na(V)1.3) Regulation of Human Cerebral Cortical Folding and Oral Motor Development. Neuron. 2018 Sep;99(5):905–913.e7.
10. Berret E, Barron T, Xu J, Debner E, Kim EJ, Kim JH. Oligodendroglial excitability mediated by glutamatergic inputs and Nav1.2 activation. Nat Commun [Internet]. 2017;8(1). Available from: https://doi.org/10.1038/s41467-017-00688-0
11. Brunklaus A, Du J, Steckler F, Ghanty II, Johannesen KM, Fenger CD, et al. Biological concepts in human sodium channel epilepsies and their relevance in clinical practice. Epilepsia. 2020;61(3):387–99. https://doi.org/10.1111/epi.16438.
12. Kang HJ, Kawasawa YI, Cheng F, Zhu Y, Xu X, Li M, et al. Spatio-temporal transcriptome of the human brain. Nature [Internet]. 2011;478(7370):483–9. Available from: http://www.ncbi.nlm.nih.gov/pubmed/22031440
13. Wolff M, Johannesen KM, Hedrich UBS, Masnada S, Rubboli G, Gardella E, et al. Genetic and phenotypic heterogeneity suggest therapeutic implications in SCN2A-related disorders. Brain [Internet]. 2017; Available from: https://academic.oup.com/brain/article-lookup/doi/10.1093/brain/awx054
14. Tian C, Wang K, Ke W, Guo H, Shu Y. Molecular identity of axonal sodium channels in human cortical pyramidal cells. Front Cell Neurosci [Internet]. 2014;8(September):297. Available from: http://journal.frontiersin.org/article/10.3389/fncel.2014.00297/abstract
15. Plummer NW, McBurney MW, Meisler MH. Alternative splicing of the sodium channel SCN8A predicts a truncated two-domain protein in fetal brain and non-neuronal cells. J Biol Chem. 1997;272(38):24008–15. https://doi.org/10.1074/jbc.272.38.24008.
16. Gustafson TA, Clevinger EC, Neill TJO, Yarowskys PJ, Kruegerg BK. Mutually exclusive exon splicing of type III brain sodium channel alpha subunit RNA generates developmentally regulated isoforms in rat brain. J Biol Chem. 1993;268(25):18648–53. https://doi.org/10.1016/S0021-9258(17)46679-8.
17. Zaman T, Helbig KL, Clatot J, Thompson CH, Kang SK, Stouffs K, et al. SCN3A-Related Neurodevelopmental Disorder: A Spectrum of Epilepsy and Brain Malformation. Ann Neurol. 2020 Jun;
18. Zaman T, Helbig I, Božović IB, DeBrosse SD, Bergqvist AC, Wallis K, et al. Mutations in SCN3A cause early infantile epileptic encephalopathy. Ann Neurol. 2018 Apr;83(4):703–17. https://doi.org/10.1002/ana.25188.
19. Liao Y, Deprez L, Maljevic S, Pitsch J, Claes L, Hristova D, Jordanova A, Ala-Mello S, Bellan-Koch A, Blazevic D, Schubert S, Thomas EA, Petrou S, Becker AJ, de Jonghe P, Lerche H Molecular correlates of age-dependent seizures in an inherited neonatal-infantile epilepsy. Brain [Internet] 2010;133(5):1403–1414. Available from: http://www.brain.oxfordjournals.org/cgi/doi/10.1093/brain/awq057
20. Gazina E V, Richards KL, Mokhtar MBC, Thomas E, Reid C, Petrou S. Differential expression of exon 5 splice variants of sodium channel alpha subunit mRNAs in the developing mouse brain. Neuroscience [Internet]. 2010;166(1):195–200. Available from: http://www.ncbi.nlm.nih.gov/pubmed/20006674
21. Tate SK, Depondt C, Sisodiya SM, Cavalleri GL, Schorge S, Soranzo N, et al. Genetic predictors of the maximum doses patients receive during clinical use of the anti-epileptic drugs carbamazepine and phenytoin. Proc Natl Acad Sci U S A. 2005;102(15):5507–12. https://doi.org/10.1073/pnas.0407346102.
22. Tate SK, Singh R, Hung CC, Tai JJ, Depondt C, Cavalleri GL, et al. A common polymorphism in the SCN1A gene associates with phenytoin serum levels at maintenance dose. Pharmacogenet Genomics. 2006;16(10):721–6. https://doi.org/10.1097/01.fpc.0000230114.41828.73.
23. O'Brien JE, Drews VL, Jones JM, Dugas JC, Barres BA, Meisler MH. Rbfox proteins regulate alternative splicing of neuronal sodium channel SCN8A. Mol Cell Neurosci [Internet] 2012;49(2):120–126. Available from: https://doi.org/10.1016/j.mcn.2011.10.005
24. Thompson CH, Ben-Shalom R, Bender KJ, George AL. Alternative splicing potentiates dysfunction of early-onset epileptic encephalopathy SCN2A variants. J Gen Physiol. 2020;152(3):1–16.
25. Kasai N, Fukushima K, Ueki Y, Prasad S, Nosakowski J, Sugata KI, et al. Genomic structures of SCN2A and SCN3A - Candidate genes for deafness at the DFNA16 locus. Gene. 2001;264(1):113–22. https://doi.org/10.1016/S0378-1119(00)00594-1.
26. Copley RR. Evolutionary convergence of alternative splicing in ion channels. Trends Genet. 2004;20(4):171–6. https://doi.org/10.1016/j.tig.2004.02.001.
27. Xu R, Thomas EA, Jenkins M, Gazina EV, Chiu C, Heron SE, et al. A childhood epilepsy mutation reveals a role for developmentally regulated splicing of a sodium channel. Mol Cell Neurosci. 2007;35(2):292–301. https://doi.org/10.1016/j.mcn.2007.03.003.
28. Gazina EV, Leaw BTWW, Richards KL, Wimmer VC, Kim TH, Aumann TD, et al. "Neonatal" Nav1.2 reduces neuronal excitability and affects seizure susceptibility and behaviour. Hum Mol Genet. 2015;24(5):1457–68. https://doi.org/10.1093/hmg/ddu562.
29. Thompson CH, Kahlig KM, George AL. SCN1A splice variants exhibit divergent sensitivity to commonly used antiepileptic drugs. Epilepsia. 2011; 52(5):1000–9. https://doi.org/10.1111/j.1528-1167.2011.03040.x.
30. Diss JKJ, Fraser SP, Djamgoz MBA. Voltage-gated Na+ channels: Multiplicity of expression, plasticity, functional implications and pathophysiological aspects. Eur Biophys J. 2004;33(3):180–93.
31. Zubović L, Baralle M, Baralle FE. Mutually exclusive splicing regulates the Nav 1.6 sodium channel function through a combinatorial mechanism that

Liang *et al. Genome Medicine* (2021) 13:135

Page 14 of 14

involves three distinct splicing regulatory elements and their ligands. Nucleic Acids Res. 2012;40(13):6255–69. https://doi.org/10.1093/nar/gks249.

32. Harrow J, Frankish A, Gonzalez JM, Tapanari E, Diekhans M, Kokocinski F, et al. GENCODE: the reference human genome annotation for The ENCODE Project. Genome Res [Internet]. 2012;22(9):1760–74. Available from: http://www.ncbi.nlm.nih.gov/pubmed/22955987

33. Werling DM, Pochareddy S, Choi J, An J-YY, Sheppard B, Peng M, et al. Whole-Genome and RNA Sequencing Reveal Variation and Transcriptomic Coordination in the Developing Human Prefrontal Cortex. Cell Rep. 2020 Apr;31(1):107489. https://doi.org/10.1016/j.celrep.2020.03.053.

34. Li M, Santpere G, Kawasawa YI, Evgrafov OV, Gulden FO, Pochareddy S, et al. Integrative functional genomic analysis of human brain development and neuropsychiatric risks. Science. 2018;362:6420.

35. MacLaren R, Radcliffe RA, Van Matre ET, Robertson CE, Ir D, Frank DN. The Acute Influence of Acid Suppression with Esomeprazole on Gastrointestinal Microbiota and Brain Gene Expression Profiles in a Murine Model of Restraint Stress. Neuroscience [Internet]. 2019;398:206–17. Available from: https://doi.org/10.1016/j.neuroscience.2018.11.048, 2019

36. Dobin A, Davis CA, Schlesinger F, Drenkow J, Zaleski C, Jha S, et al. STAR: ultrafast universal RNA-seq aligner. Bioinformatics. 2013 Jan;29(1):15–21. https://doi.org/10.1093/bioinformatics/bts635.

37. Anders S, Reyes A, Huber W. Detecting differential usage of exons from RNA-seq data. Genome Res. 2012;22(10):2008–17. https://doi.org/10.1101/gr.133744.111.

38. Bedre R. reneshbedre/bioinfokit: Bioinformatics data analysis and visualization toolkit. 2020 Jul 29 [cited 2020 Sep 10]; Available from: https://doi.org/10.5281/zenodo.3965241#.X1p62G7zZyE.mendeley

39. Karimzadeh M, Ernst C, Kundaje A, Hoffman MM. Umap and Bismap: quantifying genome and methylome mappability. Nucleic Acids Res. 2018 Nov;46(20):e120. https://doi.org/10.1093/nar/gky677.

40. Wu J, Anczukow O, Krainer AR, Zhang MQ, Zhang C. OLego: fast and sensitive mapping of spliced mRNA-Seq reads using small seeds. Nucleic Acids Res. 2013 May;41(10):5149–63. https://doi.org/10.1093/nar/gkt216.

41. Li YI, Knowles DA, Humphrey J, Barbeira AN, Dickinson SP, Im HK, et al. Annotation-free quantification of RNA splicing using LeafCutter. Nat Genet. 2018 Jan;50(1):151–8. https://doi.org/10.1038/s41588-017-0004-9.

42. An J-Y, Lin K, Zhu L, Werling DM, Dong S, Brand H, et al. Genome-wide de novo risk score implicates promoter variation in autism spectrum disorder. Science. 2018;362(6420):eaat6576.

43. Ongen H, Buil A, Brown AA, Dermitzakis ET, Delaneau O. Fast and efficient QTL mapper for thousands of molecular phenotypes. Bioinformatics. 2016 May;32(10):1479–85. https://doi.org/10.1093/bioinformatics/btv722.

44. Benjamini Y, Hochberg Y. Controlling the False Discovery Rate: A Practical and Powerful Approach to Multiple Testing. J R Stat Soc Ser B. 1995;57(1):289–300.

45. Nowakowski TJ, Bhaduri A, Pollen AA, Alvarado B, Mostajo-Radji MA, Di Lullo E, et al. Spatiotemporal gene expression trajectories reveal developmental hierarchies of the human cortex. Forensic Sci Int 2017;358(6368):1318–1323. Available from: http://www.sciencemag.org/lookup/doi/10.1126/science.aap8809

46. Tang L, Lu X, Tao Y, Zheng J, Zhao P, Li K, et al. SCN1A rs3812718 polymorphism and susceptibility to epilepsy with febrile seizures: a meta-analysis. Gene. 2014 Jan;533(1):26–31. https://doi.org/10.1016/j.gene.2013.09.071.

47. Wang ZJ, Chen J, Chen HL, Zhang LY, Xu D, Jiang WT. Association between SCN1A polymorphism rs3812718 and valproic acid resistance in epilepsy children: a case-control study and meta-analysis. Biosci Rep. 2018 Dec;38(6).

48. The International League Against Epilepsy Consortium on Complex Epilepsies. Genome-wide mega-analysis identifies 16 loci and highlights diverse biological mechanisms in the common epilepsies. Nat Commun. 2018;9(1):5269.

49. Heinzen EL, Yoon W, Tate SK, Sen A, Wood NW, Sisodiya SM, et al. Nova2 interacts with a Cis-acting polymorphism to influence the proportions of drug-responsive splice variants of SCN1A. Am J Hum Genet. 2007;80(5):876–83. https://doi.org/10.1086/516650.

50. Jaganathan K, Kyriazopoulou Panagiotopoulou S, McRae JF, Darbandi SF, Knowles D, Li YI, et al. Predicting Splicing from Primary Sequence with Deep Learning. Cell [Internet]. 2019;0(0):1–14. Available from: https://linkinghub.elsevier.com/retrieve/pii/S0092867418316295

51. GTEx Consortium. Human genomics. The Genotype-Tissue Expression (GTEx) pilot analysis: multitissue gene regulation in humans. Science [Internet]. 2015;348(6235):648–60. Available from: http://www.ncbi.nlm.nih.gov/pubmed/25954001

52. Finkel RS, Mercuri E, Darras BT, Connolly AM, Kuntz NL, Kirschner J, et al. Nusinersen versus Sham Control in Infantile-Onset Spinal Muscular Atrophy. N Engl J Med [Internet]. 2017/11/02. 2017;377(18):1723–32. Available from: https://www.ncbi.nlm.nih.gov/pubmed/29091570

53. Kim J, Hu C, Moufawad El Achkar C, Black LE, Douville J, Larson A, et al. Patient-Customized Oligonucleotide Therapy for a Rare Genetic Disease. N Engl J Med. 2019 Oct;381(17):1644–52. https://doi.org/10.1056/NEJMoa1813279.

54. Lenk GM, Jafar-Nejad P, Hill SF, Huffman LD, Smolen CE, Wagnon JL, et al. Scn8a Antisense Oligonucleotide Is Protective in Mouse Models of SCN8A Encephalopathy and Dravet Syndrome. Ann Neurol. 2020;87(3):339–46. https://doi.org/10.1002/ana.25676.

55. Han Z, Chen C, Christiansen A, Ji S, Lin Q, Anumonwo C, et al. Antisense oligonucleotides increase Scn1a expression and reduce seizures and SUDEP incidence in a mouse model of Dravet syndrome. Sci Transl Med. 2020;12(558).

56. Li M, Jancovski N, Jafar-Nejad P, Burbano LE, Rollo B, Richards K, et al. Antisense oligonucleotide therapy for SCN2A gain-of-function epilepsy. bioRxiv [Internet]. 2020 Jan 1;2020.09.09.289900. Available from: http://biorxiv.org/content/early/2020/09/11/2020.09.09.289900.abstract

57. Berkovic SF, Grinton B, Dixon-Salazar T, Laughlin BL, Lubbers L, Milder J, et al. De novo variants in the alternative exon 5 of SCN8A cause epileptic encephalopathy. Genet Med. 2018;20(2):275–81.

58. Sanders SJ, Campbell AJ, Cottrell JR, Moller RS, Wagner FF, Auldridge AL, et al. Progress in Understanding and Treating SCN2A-Mediated Disorders. Trends Neurosci. 2018;41:442–56.

59. Ben-Shalom R, Keeshen CM, Berrios KN, An JY, Sanders SJ, Bender KJ. Opposing effects on NaV1.2 function underlie differences between SCN2A variants observed in individuals with autism spectrum disorder or infantile seizures. Biol Psychiatry [Internet]. 2017 Feb 11 [cited 2017 Nov 30];82(3):1–9. Available from: https://doi.org/10.1016/j.biopsych.2017.01.009, 82, 3, 224, 232

60. Spratt PWE, Alexander RPD, Ben-Shalom R, Sahagun A, Kyoung H, Keeshen CM, Sanders SJ, Bender KJ. Paradoxical hyperexcitability from Na(V)1.2 sodium channel loss in neocortical pyramidal cells. Cell Rep. 2021;36(5):109483.

61. Zhang J, Chen X, Eaton M, Lai S, Park A, Ahmad TS, et al. Severe deficiency of voltage-gated sodium channel Na<sub>V<sub>1.2 elevates neuronal excitability in adult mice. bioRxiv [Internet]. 2021 Jan 1;2021.02.02.429384. Available from: http://biorxiv.org/content/early/2021/02/02/2021.02.02.429384.abstract

62. Miyamoto H, Tatsukawa T, Shimohata A, Yamagata T, Suzuki T, Amano K, et al. Impaired cortico-striatal excitatory transmission triggers epilepsy. Nat Commun. 2019 Apr;10(1):1917. https://doi.org/10.1038/s41467-019-09954-9.

63. Wagnon JL, Barker BS, Ottolini M, Park Y, Volkheimer A, Valdez P, et al. Loss-of-function variants of SCN8A in intellectual disability without seizures. Neurol Genet. 2017 Aug;3(4):e170. https://doi.org/10.1212/NXG.0000000000000170.

64. Taladriz-Sender A, Campbell E, Burley GA. Splice-switching small molecules: A new therapeutic approach to modulate gene expression. Methods. 2019 Sep;167:134–42. https://doi.org/10.1016/j.ymeth.2019.06.011.

65. Anvar SY, Allard G, Tseng E, Sheynkman GM, de Klerk E, Vermaat M, et al. Full-length mRNA sequencing uncovers a widespread coupling between transcription initiation and mRNA processing. Genome Biol. 2018;19(1):1–18.

66. Clark MB, Wrzesinski T, Garcia AB, Hall NAL, Kleinman JE, Hyde T, Weinberger DR, Harrison PJ, Haerty W, Tunbridge EM Long-read sequencing reveals the complex splicing profile of the psychiatric risk gene CACNA1C in human brain. Mol Psychiatry [Internet] 2020;25(1):37–47. Available from: https://doi.org/10.1038/s41380-019-0583-1

67. Gupta I, Collier PG, Haase B, Mahfouz A, Joglekar A, Floyd T, et al. Single-cell isoform RNA sequencing characterizes isoforms in thousands of cerebellar cells. Nat Biotechnol. 2018 Oct;

68. Liang L, Sanders SJ. Splicing analysis code [Internet]. 2021. Available from: https://github.com/sanderslab/splicing-pipeline-containers

Publisher's Note